Scavenger receptor BI promotes cytoplasmic accumulation of lipoproteins in clear-cell renal cell carcinoma

Velagapudi, Srividya ; Schraml, Peter ; Yalcinkaya, Mustafa ; Bolck, Hella Anna ; Rohrer, Lucia ; Moch, Holger ; von Eckardstein, Arnold

Abstract: Clear cell renal cell carcinomas (ccRCC) are characterized by inactivation of von Hippel-Lindau (VHL) gene and intracellular lipid accumulation by unknown pathomechanism. The immunochemical analysis of 356 RCCs revealed high abundance of apolipoproteins apoA-I and apoB as well as scavenger receptor BI (SR-BI) in the clear cell RCC subtype. Given the characteristic loss of VHL function in ccRCC, we used VHL-defective and VHL-proficient cells to study the potential influence of VHL on lipoprotein uptake. VHL-defective patient-derived ccRCC cells and cell lines (786O and RCC4) showed enhanced uptake as well as less re-secretion and degradation of radio-iodinated high and low density lipoproteins (125I-HDL and 125I-LDL) compared to the VHL-proficient cells. The ccRCC cells showed enhanced VEGF and SR-BI expression compared to normal kidney epithelial cells. Uptake of 125I-HDL and 125I-LDL by patient-derived normal kidney epithelial cells as well as VHL-re-expressing ccRCC cell lines 786-O-VHL and RCC4-O-VHL cells was strongly enhanced by VEGF treatment. The knock-down of VEGF co-receptor neuropilin (NRP1) as well as blocking of SR-BI significantly reduced the uptake of lipoproteins into ccRCC cells in vitro. LDL stimulated proliferation of 786-O cells more potently than 786-O-VHL cells in a NRP1- and SR-BI- dependent manner. In conclusion, enhanced lipoprotein uptake due to increased activities of VEGF/NRP1 and SR-BI promotes lipid accumulation and proliferation of VHL-defective ccRCC cells.

DOI: https://doi.org/10.1194/jlr.M083311

Scavenger receptor BI promotes cytoplasmic accumulation of lipoproteins in clear-cell renal cell carcinoma

Srividya Velagapudi[1], Peter Schraml[2], Mustafa Yalcinkaya[1], Hella A. Bolck[2], Lucia Rohrer[1], Holger Moch[2,*], and Arnold von Eckardstein[1,*]

***: equal contribution**

Institute of Clinical Chemistry[1] and Department of Pathology and Molecular Pathology[2], University of Zurich and University Hospital of Zurich, Switzerland

Running title: SR-BI induces lipid accumulation in ccRCC

Correspondence to:

Arnold von Eckardstein, MD University Hospital Zurich

Institute of Clinical Chemistry

Raemistrasse 100

CH 8091 ZURICH

Switzerland

phone: +41 44 255 2260

fax: +41 44 255 4590

email: arnold.voneckardstein@usz.ch

Conflict of interest: None

Word count of main text: 5587

Abstract (215 words)

Clear cell renal cell carcinomas (ccRCC) are characterized by inactivation of von Hippel-Lindau (VHL) gene and intracellular lipid accumulation by unknown pathomechanism. The immunochemical analysis of 356 RCCs revealed high abundance of apolipoproteins apoA-I and apoB as well as scavenger receptor BI (SR-BI) in the clear cell RCC subtype. Given the characteristic loss of VHL function in ccRCC, we used VHL-defective and VHL-proficient cells to study the potential influence of VHL on lipoprotein uptake. VHL-defective patient-derived ccRCC cells and cell lines (786O and RCC4) showed enhanced uptake as well as less re-secretion and degradation of radio-iodinated high and low density lipoproteins (^{125}I-HDL and ^{125}I-LDL) compared to the VHL-proficient cells. The ccRCC cells showed enhanced VEGF and SR-BI expression compared to normal kidney epithelial cells. Uptake of ^{125}I-HDL and ^{125}I-LDL by patient-derived normal kidney epithelial cells as well as VHL-re-expressing ccRCC cell lines 786-O-VHL and RCC4-O-VHL cells was strongly enhanced by VEGF treatment. The knock-down of VEGF co-receptor neuropilin (NRP1) as well as blocking of SR-BI significantly reduced the uptake of lipoproteins into ccRCC cells *in vitro*. LDL stimulated proliferation of 786-O cells more potently than 786-O-VHL cells in a NRP1- and SR-BI- dependent manner. In conclusion, enhanced lipoprotein uptake due to increased activities of VEGF/NRP1 and SR-BI promotes lipid accumulation and proliferation of VHL-defective ccRCC cells.

Keywords

Clear-cell renal cell carcinoma, LDL, HDL, Vascular endothelial growth factor, Scavenger receptor class B-I

Introduction

Classification of renal cell carcinomas (RCC) subtypes is based on histologically predominant cytoplasmic features (clear cell RCC, ccRCC), characteristic staining (chromophobe RCC), architectural features (papillary RCC) or specific molecular alterations (translocation RCC). CcRCC, received its name from the microscopic appearance upon staining of formalin fixed and paraffin embedded (FFPE) sections with hematoxylin-eosin (1). The clear appearance of the cytoplasm is due to the accumulation of glycogen and lipids that are dissolved during routine processing with deparaffinization of FFPE sections using xylene and ethanol. The most prominent lipid stored in renal tumor cells is cholesterol, largely in the esterified form (2). The mechanisms for cholesterol accumulation in ccRCC cells is not well understood. Three principle pathways have to be considered, two of which have been ruled out previously, namely excessive cholesterol synthesis by the finding of decreased rather than increased activity of the rate limiting enzyme HMG-CoA reductase (3) as well as abnormal cholesterol efflux (2). The third explanation is most likely, excessive uptake of cholesterol from plasma lipoproteins beyond the capacity of utilization and processing. However, neither the lipoprotein classes nor the receptors and cellular pathways involved are well characterized. CcRCC lacks the low-density lipoprotein receptor (LDLR), which is the main entry route for exogenous cholesterol into the majority of cells including many tumor cells (4). In contrast, the expression of both the very low-density lipoprotein receptor (VLDLR) and scavenger receptor-BI (SR-BI) was found increased in ccRCC compared to the normal kidney tissue (5) and to mediate lipid uptake into ccRCC cells from very low density lipoproteins (VLDL) and high density lipoproteins (HDL), respectively (5, 6).

The activity of vascular endothelial growth factor (VEGF) is increased in the majority of ccRCCs (7, 8) due to the constitutive activation of hypoxia-inducible factor 1 alpha (HIF-1α) by somatic mutations in the von Hippel-Lindau (*VHL*) tumor suppressor gene. The VHL protein is a component of the E3-ubiquitin ligase complex that ubiquitylates HIF-1α and HIF-2α for proteasome-mediated degradation (7-9). Thus, the loss of *VHL* function leads to HIF-1α stabilization despite an adequately oxygenated tissue microenvironment, which in turn results in uncontrolled activation of HIF-target genes that regulate erythropoiesis (erythropoietin), angiogenesis (VEGF), glycolysis (glucose transporters and

glycolytic pathway enzymes), and apoptosis (BNIP3)(8-12). We have previously found that VEGF promotes the cell surface abundance of SR-BI in endothelial cells and thereby enhances the uptake of HDL into endothelial cells (13). Therefore, we hypothesized that increased activities of HIF-1α and hence VEGF promote the cell surface expression of SR-BI and thereby uptake of HDL. To test this hypothesis, we combined immunohistochemical studies in human renal tumors with experiments in two ccRCC model cell lines and patient-derived ccRCC cell cultures.

Materials and Methods

Patients, Tissue microarray Construction and Immunohistochemistry

RCC patients were identified from the database of the Institute of Pathology and Molecular Pathology, University Hospital Zurich, Switzerland. All RCCs were histologically re-evaluated by one pathologist (H.M.) and selected on the basis of hematoxylin and eosin-stained tissue sections. The patient cohort and the construction of tissue microarrays (TMA) of RCC were previously described (14) (15). Tumors were staged and histologically classified according to the World Health Organization classification (16). Overall survival data were obtained by the Cancer Registry of the Canton Zurich. The clinical and pathologic parameters of the tumors on the TMA are summarized in Supplementary Table S1. For some cases there was no information available. This study was approved by the local commission of ethics (KEK-ZH no. 2011-0072/4).

TMA sections (2.5 μm) were transferred to glass slides followed by immunohistochemical analysis according to the Ventana (Tucson, AZ, USA) automat protocols and antibodies used are listed in Supplementary Table S2. The staining intensities were classified as absent (0), weak (1), moderate (2), and strong (3). For detailed analysis, TMAs were scanned using the NanoZoomer Digital Slide Scanner (Hamamatsu Photonics K.K.).

Cell culture

Tissue samples of patients were made available by the Tissue Biobank of the Department of Pathology and Molecular Pathology, University Hospital of Zurich, Switzerland upon approval of the local ethics commission (KEK-ZH-Nr. 2011-0072 and KEK-ZH-Nr. 2014-0614) and upon patients' written consent.

HE-stained sections of formalin-fixed paraffin-embedded (FFPE) and fresh frozen renal tissue specimens were reviewed by a pathologist with specialization in uropathology (H.M). Sanger sequencing was employed to assess the mutation status of the *VHL* gene (c.341-1G>C) for the ccRCC primary tumor and the corresponding cell culture. DNA was isolated from FFPE punches from tumor tissue (3 cylinders with a diameter of 0.6 mm) or a minimum of 10000 cultured cells using the Maxwell® 16 DNA Purification Kits (Promega, Madison, WI). PCR and sequencing of *VHL* was performed as previously described (17). Fresh tissue samples were placed into sterile 50 mL conical tubes containing transport media (RPMI (Gibco, Waltham, MA) with 10 % fetal calf serum (FCS, Gibco) and Antibiotic-Antimycotic® (Gibco). FFPE cell pellets from cultured cells were prepared as previously described (18) and compared to FFPE-specimens of the corresponding primary tumor by IHC. Cultures were maintained in K1 medium (19, 20) supplemented with 0.5 % FCS (Gibco) and Epinephrine (Sigma-Aldrich, St. Louis, MO) and transferred into collagen I-coated cell culture dishes (Corning, NY) in a humidified incubator at 37 °C with 5% CO_2.

The ccRCC-derived 786-O cells which lack functional pVHL were supplied by American Type Culture Collection (ATCC) and cultured in RPMI-1640 (Sigma, R8758) with 10% fetal bovine serum (Gibco) and 100U/mL of penicillin and 100µg/mL streptomycin (Sigma-Aldrich). Stable transfectant of 786-O re-expressing pVHL-isoform 30 (786-O-VHL) was provided by Prof. Dr. Wilhelm Krek (ETH, Zurich), generated as described (21) and cultured using the same conditions as mentioned for 786-O. 0.5 mg/mL of G418 (Gibco, 10131) was used as selection antibiotic. Both cell lines were authenticated by authentication service of Microsynth (Balgach, Switzerland) and were previously used by our group (22, 23).

Human aortic endothelial cells (HAECs) from Cell Applications Inc (304-05a), were cultured in endothelial cell basal medium (LONZA Clonetics CC-3156) with 5% fetal bovine serum (GIBCO), 100U/mL of penicillin and 100µg/mL streptomycin (Sigma-Aldrich), supplemented with singleQuots (LONZA Clonetics CC-4176 or ATCC PCS-100-041). Hepatocellular carcinoma cells (Huh7) from JCRB (0403), and human renal proximal tubular epithelial cell line HK-2 (provided by R. Wüthrich Clinic for Nephrology, Department of Internal Medicine, University Hospital Zurich, Switzerland) were

cultured in Dulbecco's Modified Eagle Medium (DMEM) with 10% fetal bovine serum (Gibco) and 100U/mL of penicillin and 100µg/mL streptomycin (Sigma-Aldrich).

Lipoprotein Isolation and labeling

LDL (1.019<d<1.063 g/mL) and HDL (1.063<d<1.21 g/mL) were isolated from fresh normolipidemic plasma of blood donors by sequential ultracentrifugation as described previously (24, 25). LDL and HDL were radioiodinated with $Na^{125}I$ by the McFarlane monochloride procedure modified for lipoproteins (25, 26). Specific activities between 300-900 cpm/ng of protein were obtained.

Lipoprotein cell association, pulse-chase and degradation assays

All assays were performed in RPMI-1640 (Sigma) containing 25mmol/L HEPES and 0.2% BSA instead of serum (referred to as assay medium). Where indicated, cells were pre-treated with Sorafenib Tosylate (Selleckchem, 90nM) or Sunitinib Malate (Selleckchem, 80nM) for 30 minutes or with VEGF-A (Sigma, 25ng/mL) or anti-SR-BI neutralizing antibody (1:500, Novus NB400-113) or anti-IgG control (1:500, Santa Cruz-2027) for 1 hour at 37 ºC. Following treatments, the cells were incubated with 10µg/mL of ^{125}I-HDL or ^{125}I-LDL in the absence or presence of a 40 times excess of non-labeled HDL and LDL respectively for 1 hour at 37ºC for association experiments. At the end of cell association step, the cells were washed twice with Tris- BSA buffer, followed by two washes with PBS containing $CaCl_2$ and $MgCl_2$ and then lysed in 0.1N NaOH buffer. Specific cellular association was calculated by subtracting the values obtained in the presence of excess unlabeled HDL or LDL (unspecific) from those obtained in the absence of unlabeled HDL and LDL (total) respectively

For pulse-chase experiments, 50,000 cells were seeded in 24 wells plates and cultured for 48 hours. Then the cells were pulsed for 1 hour with 10µg/mL of ^{125}I-HDL or ^{125}I-LDL at 37 ºC in the presence or absence of the respective unlabeled lipoprotein for competition and determination of specific interactions. After 1 hour of pulse incubation, the cells were either directly processed for the measurement of association or were washed three times with assay medium, chased for 1, 2 or 4 hours at 37 ºC with the assay medium containing 10µg/ml of unlabeled HDL or LDL. At the end of each chase period, the cells were handled as described above for the cellular association experiments. In addition, the media were collected and subjected to precipitation with trichloroacetic acid (TCA). Radioactivity

was counted by Perkin Elmer γ-counter. Precipitated radioactivity was postulated to reflect non-degraded lipoproteins whereas radioactivity in the supernatant was considered to reflect degraded lipoproteins. (27). The amount of radioactivity in each fraction of the well (cell associated, TCA supernatant and TCA precipitated) was calculated by normalizing to the specific cellular association of the no chase of parental 786-O cells or primary ccRCC cells (represents initial radioactivity for the chase points).

Real-time polymerase chain reaction

Total RNA was isolated using TRI reagent (Sigma T9424) according to the manufacturer's instruction. Genomic DNA was removed by digestion using DNase (Roche) and RNase inhibitor (Ribolock, Thermo Scientific). Reverse transcription was performed using M-MLVRT (Invitrogen, 200U/μL) following the standard protocol as described by the manufacturer. Quantitative PCR was done with Lightcycler FastStart DNA Master SYBR Green I (Roche) using gene specific primers as mentioned in the Supplementary information.

Small interfering RNA transfection

786-O and 786-O-VHL cells were reverse transfected with small interfering RNA (Ambion silencer select, Life technologies) targeted to LDLR (s224006, s224007, s4) or VLDLR (siGENOME SMARTpool siRNA D-003721-02; ON-TARGET plus human VLDLR (7436), Dharmacon) or NRP1 (s16844, s16843) or non-silencing control (4390843, silencer select or siGENOME control siRNA D-001220-01-20, Dharmacon or ON-TARGET control siRNA D-01810-10-20, Dharmacon) at a final concentration of 5nmol/L using Lipofectamine RNA iMAX transfection reagent (Invitrogen, 13778150) in an antibiotic-free medium. All experiments were performed 72 hours post-transfection and efficiency of transfection was confirmed with atleast two siRNAs against each gene using qRT-PCR.

Western Blotting

Cells were lysed in RIPA buffer (10mmol/L Tris pH 7.4, 150mmol/L NaCl, 1% NP-40, 1% sodium deoxycholate, 0.1% SDS, complete EDTA (Roche)) with protease inhibitors (Roche). Equal amounts of protein were separated on SDS-PAGE and trans-blotted onto PVDF membrane (GE Healthcare).

Membranes were blocked in appropriate blocking buffer recommended for the antibody (TBS-T supplemented with 5% milk) and incubated overnight on a shaker at 4 ºC with primary antibodies in the same blocking buffer. Membranes were incubated for 1 hour with an HRP-conjugated secondary antibody (Dako) in the blocking buffer. Membranes were further incubated with chemiluminescence substrate for 1min (Pierce ECL plus, Thermo scientific) and imaged using Fusion Fx (Vilber). The expression of LDLR (1:1000, ab30532, Abcam), VLDLR (1:1000, Novus, NBP1-78162), SR-BI (1:1000, NB400-131, Novus), NRP1 (1:1000, ab81321, Abcam) were evaluated and compared to the expression of either TATA binding protein (1:1000, TBP, ab51841, Abcam) which was used as a loading control.

Cell surface expression analysis

Biotinylation of intact cells was performed using 20mg/mL EZ-Link sulfo-NHS-S-S-Biotin (Thermo Scientific) in the cold for 1 hour with mild shaking and quenched with ice-cold 50mM Tris pH 7.4. Cells were lysed in RIPA buffer (total cell lysate) and 200-500µg of lysates were incubated with 20µL of BSA-blocked streptavidin beads suspension (GE Healthcare) for 16 hours at 4 ºC and pelleted by centrifugation; the pellet represents surface proteins. Proteins were dissociated from the pellet by boiling with SDS loading buffer and analyzed by SDS-PAGE and immunoblotted with SR-BI antibody (NB400-131, Novus), TATA binding protein (TBP, ab51841, Abcam) used as intracellular control and Na^+/K^+-ATPase (1:200, Santa Cruz-21712) used as cell surface control.

Cell proliferation assay

Cells were cultured at a density of 5000 cells per well in a 96 well plate for 72 hours. After transfecting with either siRNA against NRP1 or LDLR or non-silencing controls for 60 hours or blocking with SR-BI neutralizing antibody for 1 hour, the cells were treated overnight with 50µg/mL of HDL or LDL. Following the overnight treatment, the supernatant was removed and cells were washed twice with PBS. The cells were then incubated with 30µL of MTT solution (5mg/mL in PBS,Sigma, M5655) diluted in 270µL of DMEM for 30 minutes. The resultant formazan salts were extracted with dimethyl sulfoxide (DMSO) and absorbance intensity was read at 550nm and reference wavelength at 650nm (DMSO). The rate of cell proliferation is calculated relative to the 786-O parental cell line.

Statistical Analysis

Contingency table analysis and Pearson's chi-square tests were used to analyze the associations between protein expression patterns and clinical parameters. Overall survival rates were determined according to the Kaplan–Meier method and analyzed for statistical differences using a log rank test.

The data sets for all *in vitro* experiments were performed with the GraphPad Prism 7.02 software. Data sets from independent experiments were pooled and the statistical tests were chosen based on the number of groups being compared (two or more than two). All the in vitro tests in this manuscript are based either on Mann-Whitney t-test or Kruskal-Wallis followed by Dunn's post-test. Values are expressed as mean±s.e.m. $P<0.05$ was regarded as significant and $P>0.05$ was regarded as no significance.

Results

Lipoprotein and apolipoprotein expression and pathological parameters

Immunostaining was performed on RCC tissue microarrays (TMA) for the major apolipoproteins of HDL and LDL, apolipoprotein A-I (apoA-I) and apolipoprotein B (apoB) respectively (Figures 1a and 1b), as well as scavenger receptor BI (SR-BI, Figure 1c). Based on the staining intensities, expression levels in tumors were graded from 0 to 3 for apoA-I and SR-BI expression, and from 0 to 2 for apoB expression as staining intensities were generally lower. Increased immunoreactivity with anti-apoA-I or anti SR-BI antibodies but not immunoreactivity with anti-apoB antibodies significantly differentiated 175 ccRCC tissues from papillary RCC (Table 1).

Strong cytoplasmic apoA-I and SR-BI expression (staining intensity 2 and 3) was seen in approximately 75% and 56% of ccRCC. Moderate and weak cytoplasmic apoB expression was observed in 78% of ccRCC. This data indicates that the presence of apolipoproteins is characteristic in the majority of ccRCC (Table 1).

We next evaluated the associations of the lipoprotein immunoreactivities in ccRCC with tumor stage (pT) and ISUP grade. Only anti-apoB-immunoreactivity was significantly associated with late tumor stage (Supplementary Table S3, $P = 0.0371$). apoA-I ($P = 0.025$) and apoB ($P = 0.0006$) but not SR-

BI expression was significantly correlated with higher ISUP grade (Supplementary Table S4). We used the Kaplan-Meier method and log-rank test to evaluate any associations of apoA-I, apoB and SR-BI immunoreactivity with overall survival (Supplementary Figure S1a-c). Only anti-apoA-I expression was significantly correlated with worse patient outcome (P = 0.0407, Supplementary Figure S1a). This association lost statistical significance upon multivariate analysis taking into account tumor stage and grade.

Expression of apolipoproteins, SR-BI, and VHL downstream targets

Loss of function of the VHL protein leads to stabilization of HIF-α in ccRCC. Therefore, we statistically evaluated the associations of lipoprotein immunoreactivity with markers of the VHL/HIF axis, namely HIF-1α (Supplementary Table S5) and HIF-1α targets CA9 and GLUT1 (Supplementary Tables S6 and S7) as well as microvessel density recorded by CD34 abundance (Supplementary Table S8). Interestingly, the immunoreactivity for apoA-I showed significant positive associations with each of the four markers (HIF-1α: P = 0.0078; CA9: P = 0.0272; GLUT1: P = 0.0175 CD34: P < 0.001). ApoB immunoreactivity was significantly and positively associated with microvessel density (P = 0.0197) and nuclear HIF-1α staining (P = 0.0049). However, SR-BI immunoreactivity showed no significant association with any marker.

ccRCC cells do not express apolipoproteins A-I and B but show enhanced uptake and impaired degradation and re-secretion of both HDL and LDL

To unravel the origin of lipoprotein accumulation in ccRCC, we performed *in vitro* assays in two ccRCC cell lines which lack functional VHL (786-O and RCC4) and their stably transfected VHL wild-type counterparts (786-O-VHL, RCC4-O-VHL). To further corroborate our findings, we utilized patient-derived ccRCC and normal epithelial kidney cell cultures that were established from surgical tissue specimens. Histological and genotypic comparison verified the resemblance of the patient-derived ccRCC and normal epithelial cell cultures to their respective primary human tissue. Immunohistochemistry of Pax8 and pan-Cytokeratin verified the renal epithelial origin of both PDC cultures while CAIX expression unequivocally confirmed the presence of malignant cells in the ccRCC

PDC culture (Supplementary Figure S2). Importantly, the ccRCC-derived cell culture retained the *VHL* driver mutation of the primary human tumor.

We first analyzed by RT-PCR whether APOA1 and APOB are expressed by patient-derived ccRCC cells or the ccRCC cell lines. The hepatocellular derived carcinoma cell line Huh7 was used as positive control, human aortic endothelial cells (HAECs) served as negative control (Supplementary Figure S3a,b). Neither patient-derived ccRCC cells nor 786-O nor RCC4 showed any APOA1 and APOB transcripts (Supplementary Figure S3). However, we found both anti-apoA-I and apoB-immunoreactivity in ccRCC tissue and patient-derived cell culture, possibly due to uptake from the serum containing cell culture media.

Both, the patient-derived ccRCC cells culture and the VHL-deficient cell lines 786-O and RCC4 showed significantly higher specific cell association of ^{125}I-HDL and ^{125}I-LDL compared to the normal kidney epithelial cells and the re-transfected counterpart cell lines 786-O-VHL and RCC4-VHL: After 1 hour of incubation and compared to cultured normal epithelial kidney cells, association of ^{125}I-HDL and ^{125}I-LDL were 50 to 100 % and 80 to 150% higher, respectively in the ccRCC-derived cell culture (first two columns of Figures 2a & 2b as well as Supplementary Figure S4a and b). The differences in cell association of ^{125}I-HDL and ^{125}I-LDL between 786-O and 786-O-VHL amounted to 40 to 200% and 70 to 100% respectively (first two columns of Figures 3a & 3b as well as Supplementary Figure S4c and d). The association of ^{125}I-HDL and ^{125}I-LDL by RCC4 and RCC4-VHL even differed by factors 5 and 10 respectively (Supplementary Figure S4e and f). This indicates that loss of pVHL correlates with increased lipoprotein uptake by ccRCC cells.

To investigate whether the increased cellular association of ^{125}I-HDL and ^{125}I-LDL by VHL-deficient cells is caused by impaired degradation or re-secretion of the cell associated lipoproteins, a combination of pulse-chase and degradation experiments were performed with ^{125}I-HDL and ^{125}I-LDL. Already after 1 hour chase, only 24% and 9% of the initially cell associated ^{125}I-HDL and ^{125}I-LDL, respectively, remained associated with cultured normal kidney epithelial cells. After 4 hours, both decreased significantly over prolonged chasing time to about 10% and 1% of the initial radioactivity, respectively. During prolonged chase, the percentage of degraded ^{125}I-HDL increased to 70% at the expense of the

non-degraded which decreased to 15% (Figure 2a, Supplementary Figure S5a). Very strikingly, in the patient-derived ccRCC cell culture, the percentage of cell associated ^{125}I-HDL was as high as 70% after 1hour chase and did not decrease significantly over prolonged chase. The percentages of degraded ^{125}I-HDL increased over time so that after 4 hours chase no radioactivity was precipitated in the medium. At any time point of chase, the radioactivity of both degraded and non-degraded ^{125}I-HDL was significantly lower in the patient-derived ccRCC compared to normal kidney cells (Figure 2a, Supplementary Figure S5a).

The radioactivity of ^{125}I-LDL in the medium of cultured normal kidney cells showed similar kinetics like that of ^{125}I-HDL except that the proportion of non-TCA-precipitable radioactivity was higher already after 1 hour chase (60%) and increased to 80% after 4 hours chase. The proportion of the non-degraded ^{125}I-LDL decreased from 30% after 1 hour chase to 15% after 4 hours chase. Compared to patient-derived normal kidney cells, the ccRCC cell culture was significantly less active in degrading ^{125}I-LDL: the non-TCA-precipitable proportion of radioactivity was only less than 15% after 1 hour chase and increased to 25% after 4 hours chase. The relative difference in TCA-precipitable radioactivity between patient-derived normal kidney and ccRCC cells was significant but less prominent (Figure 2b, Supplementary Figure S5b).

In principle, the same observations were made for the kinetics of ^{125}I-HDL and ^{125}I-LDL in a pulse chase experiment in the ccRCC cell lines 786-O and 786-O-VHL (Figure 3, Supplementary Figure S6): 786-O-VHL cells showed considerable degradation of ^{125}I-HDL and ^{125}I-LDL as well as re-secretion of ^{125}I-HDL whereas the parental 786-O failed to degrade both ^{125}I-HDL and ^{125}I-LDL. The 786-O cells also showed a strongly reduced capacity to re-secrete ^{125}I-HDL (Figure 3a&b, Supplementary Figure S6a, b). Together, these results indicate that the loss of VHL function in ccRCC cells increases-lipoprotein uptake into a non-degrading non-secretory compartment.

VEGF and NRP1 promote the cellular association of ^{125}I-HDL and ^{125}I-LDL in ccRCC

As expected, the patient-derived ccRCC cell culture as well as 786-O and RCC4 cells showed higher VEGF mRNA expression compared to patient-derived normal kidney epithelial cells, 786-O-VHL and RCC4-O-VHL cells, respectively (Supplementary Figure S7). Pre-treatment with VEGF for 1 hour

increased the cellular association of both ^{125}I-HDL as well as ^{125}I-LDL in patient-derived normal epithelial kidney cells but not in ccRCC-derived cells (Figure 4a, b). Similar observations were made in the ccRCC cell lines: The significantly lower cellular association of both ^{125}I-HDL and ^{125}I-LDL by 786-O-VHL and RCC4-O-VHL cells was increased by pre-treatment with VEGF for 1 hour to the same level as observed in 786-O (Figure 4c, d) and RCC4 cells (Supplementary Figure S8a,b), respectively, with or without treatment with VEGF. Further, supporting the crucial role of VEGF, pre-treatment of 786-O cells with VEGF receptor inhibitors for 30 minutes decreased specific cellular association of both ^{125}I-HDL and ^{125}I-LDL but had no effect in 786-O-VHL cells (Supplementary Figure S9a-d).

Interestingly, ccRCC cells expressed neither VEGFR1 nor VEGFR2 nor VEGFR3, but expressed neuropilin-1 (NRP1) which is a co-receptor of VEGFR (Supplementary Table S9). To test whether NRP1 mediates the effects of VEGF on the cellular association of radioiodinated lipoproteins *in vitro*, we targeted NRP1 using RNAi in 786-O and 786-O-VHL cells (Supplementary Figure S10a, b). Silencing of NRP1 led to decreased specific cellular association of ^{125}I-HDL as well as ^{125}I-LDL in both 786-O and 786-O-VHL cells. Interestingly, pre-treatment with VEGF for 1 hour stimulated the specific cellular association of neither ^{125}I-HDL nor ^{125}I-LDL in 786-O-VHL cells in which NRP1 was knocked-down (Figure 5a-d). In conclusion, VEGF/NRP1 mediated signaling stimulates the uptake of ^{125}I-HDL as well as ^{125}I-LDL in ccRCC.

SR-BI but neither LDLR nor VLDLR mediates cellular association of ^{125}I-HDL and ^{125}I-LDL in ccRCC

We next aimed to unravel which receptor enhances the lipoprotein uptake by ccRCC cells. We first assessed the expression of candidate receptors, LDLR, VLDLR and SR-BI *in vitro*. We found lower expression of LDLR in the 786-O cells compared to 786-O-VHL (Supplementary Figure S11a). By contrast, total lysates of 786-O and 786-O-VHL cells did not differ in SR-BI or VLDLR protein levels (Figure 6a and Supplementary Figure S12a). However, cell-surface biotinylation revealed strongly increased expression of SR-BI on the cell surface of parental 786-O cells compared to that of 786-O-VHL cells (Figure 6a). Knock-downs of LDLR and VLDLR by RNA interference efficiently suppressed protein abundance of LDLR and VLDLR, respectively (Supplementary Figures S11b, S12a), but did not

affect the cellular association of iodinated lipoproteins (Supplementary Figures S11c, S12b,c). By contrast in both 786-O and 786-O-VHL cells, the specific cellular association of ^{125}I-HDL as well as ^{125}I-LDL was significantly decreased in the presence of a neutralizing anti-SR-BI-antibody (Figures 6b,c). The neutralizing anti-SR-BI-antibody also decreased the cellular association of ^{125}I-HDL and ^{125}I-LDL by RCC4 and RCC4-O-VHL cells (Supplementary Figure S13a,b) as well as in patient-derived ccRCC and normal kidney epithelial cell cultures (Figure 7a, b). Taken together, these results indicate that the uptake of HDL and LDL by ccRCC cells depends on the cell-surface expression of SR-BI.

NRP1 and SR-BI mediate LDL-dependent proliferation of ccRCC cells

We finally investigated whether the excess cellular association and accumulation of lipoproteins contributed to the proliferation of ccRCC cells. We found higher proliferation of 786-O cells compared to 786-O-VHL, indicating that loss of VHL function increases proliferation in ccRCC cells (Figure 8a). Interestingly, pretreatment with LDL but less so HDL increased the proliferation of both ccRCC cell lines (Figure 8b). Basal as well as lipoprotein-stimulated proliferation was reduced in both 786-O- and 786-O-VHL cells by knock-down of NRP1 (Figure 8c and Supplementary Figure S14a). Both in the presence and absence of lipoproteins and in both 786-O and 786-O-VHL cells (Supplementary Figures S14b-d) the proliferation was significantly decreased by the neutralization of SR-BI (Figure 8d, Supplementary Figure S14b) but not by knock-down of LDLR (Supplementary Figures S14c, d). Together, these results indicate that LDL promotes the proliferation of ccRCC cells in a NRP1- and SR-BI- but not LDLR-dependent manner.

Discussion

By combining immunohistochemical studies of renal carcinomas with functional experiments in three ccRCC cell culture models we made several important findings on the as yet little understood mechanism and pathogenic role of intracellular lipid accumulation in ccRCC. First, the immunochemical investigation of apoA-I and apoB in renal carcinomas revealed that ccRCCs store lipoproteins rather than lipids *per se*. Second, our functional comparisons of a patient-derived ccRCC with a normal epithelial kidney cell culture as well as two VHL-defective ccRCC cell lines (786-O and RCC4) with VHL-intact derivative cell lines (786-O-VHL and RCC4-VHL, respectively) identified

enhanced uptake of LDL and HDL and subsequent impairment of degradation and re-secretion as the likely mechanism leading to intracellular lipid accumulation in ccRCC. Third, SR-BI was identified as the rate limiting lipoprotein receptor for the association of both HDL and LDL by ccRCC cells. Fourth VEGF, which is highly expressed by ccRCCs was found to promote the association of lipoproteins by ccRCC cells through activation of its non-canonical receptor NRP1. Fifth, LDL was found to promote ccRCC cell proliferation in a SR-BI- and NRP1- dependent manner.

The intracellular storage of LDL is very unusual because the internalization of LDL into other cells, notably hepatocytes, macrophages but also renal mesangial or tubular cells, is followed by degradation (27-29). Most cells internalize LDL via the LDL-receptor into clathrin-coated pits (30, 31). LDL is then trafficked into an endosomal/lysosomal route, depending on the presence or absence of PCSK9 either together or separated from the receptor (32, 33). The apoB moiety and cholesteryl esters of LDL are hydrolyzed by lysosomal proteases and acid lipase, respectively (34-36). In hepatocytes and macrophages but also other cells, any cholesteryl ester storage in lipid droplets results from the re-esterification of cholesterol in the ER after transfer from the lysosomes (37). The intracellular storage of endocytosed holoparticles hence argues against any role of LDLR for lipid storage in ccRCC. In fact, we confirmed the finding of others that LDLR is suppressed in ccRCC and ruled out by RNA interference that LDLR contributes to LDL or HDL association by ccRCC cells (Supplementary Figure S11). Internalization of apoB-containing lipoproteins by other members of the LDL receptor family, for example LRP1, LRP2, or VLDL receptor into a broad variety of cells is also followed by lysosomal degradation of both their proteins and lipids (38). Interestingly, the VLDL receptor was previously reported to be up-regulated in ccRCC and to promote lipid uptake into ccRCC cells. However, this study only recorded the uptake of VLDL-derived lipids rather than the lipoproteins' protein moiety (5). We found no difference in the expression of VLDLR between the ccRCC cell line 786-O and its VHL-expressing counterpart 786-O-VHL. Moreover, our siRNA experiments ruled out that VLDLR contribute to the uptake of LDL or HDL by ccRCC (Supplementary Figure S12)

The most likely reason for the unusual lipoprotein storage by ccRCC cells is the involvement of SR-BI. We, like others (5, 6, 39), found strong immunoreactivity of SR-BI in ccRCC but not in other renal tumors. Interestingly, Xu et al. previously reported a reduced content of HDL-cholesterol in 786-O cells

which were treated with siRNA against SR-BI (6). We here extend these previous findings by showing that the inhibition of SR-BI prevents the uptake of LDL as well as HDL into patient-derived cultured ccRCC cells as well as into the 786-O and RCC4 cell lines (Figure 6b,c & Figure 7a,b). The mechanism by which SR-BI promotes cellular lipoprotein uptake is not clear: SR-BI is traditionally regarded as a receptor which binds both HDL as well as LDL and provides bidirectional fluxes of cholesterol from these lipoproteins into cells or from the plasma membrane to the lipoprotein depending on the concentration gradient (40, 41). However, several examples have been reported where ablation or blockage of SR-BI also inhibited the uptake of lipoprotein particles. Notably, vascular endothelial cells were reported by our and other laboratories to internalize and transcytose HDL and LDL in an SR-BI dependent manner (42, 43). However, it is not clear whether SR-BI or one of its splice variants directly serve as an endocytic receptor (44, 45) or whether SR-BI only enables other pathways of endocytosis. Such indirect effects of SR-BI may include the activation of other receptors by altering the cholesterol distribution within the plasma membrane or signaling via its PDZ domain (46). SR-BI mediated endocytosis of HDL and LDL into endothelial cells is followed by re-secretion and hence allows transcytosis of lipoproteins, for example from the blood stream into the arterial wall or into the brain as well as from the extravascular tissue into the lymph (13, 47, 48). Interestingly, we here found that a patient-derived ccRCC cell culture as well as the VHL-deficient 786-O and RCC4 cell lines not only fail to degrade but also to re-secrete the internalized lipoproteins, notably HDL.

VEGF signaling, activated by loss of VHL function, appears to be the reason for the enhanced SR-BI mediated uptake of HDL and LDL into ccRCC cells: Compared to VHL-proficient cultured normal kidney cells, 786-O-VHL and RCC4-VHL cells, the VHL-deficient ccRCC-derived cell culture ,786-O and RCC4 cells show increased expression of VEGF (Supplementary Figure S7a-c). Pre-treatment with VEGF increased the uptake of both HDL and LDL by normal kidney cells as well as VHL re-transfected cells which are characterized by low endogenous VEGF expression but neither by the patient-derived ccRCC cell culture nor 786-O or RCC4 cells which already express high amounts of VEGF (Figure 4a-d, Supplementary Figure S8a, b). Conversely, lipoprotein uptake was lowered in 786-O cells by VEGFR inhibitors (Supplementary Figure S9a-d). These findings are in line with the previous report of HIF-1α -dependent lipid uptake into ccRCC (6). They are also in line with our previous observation in HAECs

where VEGF promoted the translocation of SR-BI to the cell membrane as well as the uptake and transcytosis of HDL (13). In this regard it is noteworthy to reconcile the significant correlation of VHL/HIF-1α downstream targets (Glut1 and CAIX) with immunoreactivity of both apoA-I and apoB, suggesting that increased cellular apoA-I and apoB levels are a consequence of VHL/HIF-1α signaling activation. Activated VEGF signaling in ccRCC due to increased HIF-1α activity may enhance lipoprotein uptake into the tumor not only by direct actions on tumor cells but also indirectly by promoting their transport from the circulation into the tumor tissue. VEGF is known to activate the downstream signaling by binding to VEGF receptors (49). However, we did not detect the expression of any of the three VEGF receptors in the ccRCC cells (Supplementary Table S9). Importantly, in line with previous findings (50), we detected higher expression of NRP1 in the VHL lacking 786-O cells compared to the wild type VHL expressing 786-O-VHL cells. Upon binding of VEGF, NRP1 elicits angiogenesis and tumorigenesis both dependently and independently of VEGF receptors. The enhanced uptake of HDL and LDL in 786-O-VHL cells by pre-treatment with VEGF was abrogated by the suppression of NRP1 (Figure 5). Altogether, our findings identify a novel role of NRP1 in the cholesterol accumulation of ccRCC.

Our observations provide a plausible explanation for the origin of lipid accumulation in ccRCC. However, they do not allow any conclusion on whether or not enhanced lipoprotein uptake into ccRCC has any impact on the clinical course of this disease. Excessive lipids in cancer cells are considered as markers of cancer aggressiveness (51). In line with this, immunoreactivity for apoA-I, apoB, or SR-BI was associated with the differentiation of renal carcinomas into ccRCC as well as with tumor grade (apoA-I and apoB) or tumor stage (apoB). However, expression of apoB or SR-BI showed no association with prognosis. By contrast, apoB and apoA-I immunoreactivities were associated with lower tumor stage and better survival, respectively (Supplementary Table S3 and Supplementary Figure S1). Previously, in two Chinese studies each encompassing about 100 patients, SR-BI protein and mRNA expression were found associated with the prognosis of ccRCC (6, 52). We did not replicate this observation in our larger cohort of 172 patients. However, it is important to note, that in our *in vitro* experiments the cell surface expression of SR-BI rather than the total SR-BI content was dependent of VHL and VEGF. The semi-quantitative scoring of immunostaining intensity does however not

discriminate between the larger pool of intracellular SR-BI from the smaller pool of cell surface SR-BI. Interestingly, genome-wide association studies identified a borderline significant association of the rs4765623 polymorphism in SCARB1 with ccRCC susceptibility (53) indicating a pathogenic role of SR-BI in ccRCC. In line with an oncogenic role, knock down of SR-BI was found to inhibit proliferation (Figure 9, ref (6)), colony formation, migration and invasion of ccRCC cells as well as expression and phosphorylation of Akt (6). SR-BI has also been associated with carcinogenic features in breast cancer, prostate cancer, and melanoma (54, 55).

In conclusion, we identified SR-BI mediated intracellular accumulation of intact lipoproteins as the likely origin of cholesterol accumulation and the characteristic clear cytoplasm of ccRCC. VEGF induced SR-BI cell surface translocation may be the underlying mechanism and the resulting enhanced SR-BI/lipoprotein interaction may contribute to proliferation and hence prognosis of ccRCC.

Acknowledgments

We thank Silvija Radosavljevic for lipoprotein isolation and biobank team and *in situ* laboratory, in particular Adriana von Teichman, Elisabeth Göbel, Katharina Mühlbauer, Susanne Dettwiler, André Fitsche and Christiane Mittmann, for excellent technical assistance.

Author contributions

A.v.E. and H.M. developed the rationale and concept of the entire study and provided funding. H.M, P.S. and H.A.B. designed and performed the human ccRCC tissue micro array experiments as well as their statistical analysis and interpretation. H.A.B. obtained and characterized the primary cells. S.V and A.v.E designed the *in vitro* experiments and interpreted the data. S.V and M.Y performed the *in vitro* experiments as well as statistical data analysis. S.V. and A.v.E. wrote the first version of both the original and revised manuscript which was then revised by input of P.S, H.A.B , L.R and H.M.

Source of Funding

This work was supported by grants from the Swiss National Science Foundation (31003A-160126), the 7th Framework Program of the European Commission ("TransCard"; project number 603091), and the Systems X-Program ("HDL-X"; project number MRD 2014/267) to AvE as well as from the Swiss National Science Foundation (310030_166391/1), the University Research Priority Program (URPP) in Translational Cancer Research, the Kanton Zürich (Hochspezialisierte Medizin) and the Commission of Technology and Innovation (CTI, project number 18547) to H.M.

References

1. Lopez, J. I. 2013. Renal tumors with clear cells. A review. *Pathol Res Pract* **209**: 137-146.

2. Gebhard, R. L., R. V. Clayman, W. F. Prigge, R. Figenshau, N. A. Staley, C. Reesey, and A. Bear. 1987. Abnormal cholesterol metabolism in renal clear cell carcinoma. *J Lipid Res* **28**: 1177-1184.

3. Wiley, M. H., M. M. Howton, and M. D. Siperstein. 1977. The quantitative role of the kidneys in the in vivo metabolism of mevalonate. *J Biol Chem* **252**: 548-554.

4. Clayman, R. V., L. E. Bilhartz, D. K. Spady, L. M. Buja, and J. M. Dietschy. 1986. Low density lipoprotein-receptor activity is lost in vivo in malignantly transformed renal tissue. *FEBS Lett* **196**: 87-90.

5. Sundelin, J. P., M. Stahlman, A. Lundqvist, M. Levin, P. Parini, M. E. Johansson, and J. Boren. 2012. Increased expression of the very low-density lipoprotein receptor mediates lipid accumulation in clear-cell renal cell carcinoma. *PLoS One* **7**: e48694.

6. Xu, G. H., N. Lou, H. C. Shi, Y. C. Xu, H. L. Ruan, W. Xiao, L. Liu, X. Li, H. B. Xiao, B. Qiu, L. Bao, C. F. Yuan, Y. L. Zhou, W. J. Hu, K. Chen, H. M. Yang, and X. P. Zhang. 2018. Up-regulation of SR-BI promotes progression and serves as a prognostic biomarker in clear cell renal cell carcinoma. *BMC Cancer* **18**: 88.

7. Masson, N., and P. J. Ratcliffe. 2014. Hypoxia signaling pathways in cancer metabolism: the importance of co-selecting interconnected physiological pathways. *Cancer Metab* **2**: 3.

8. Hakimi, A. A., E. Reznik, C. H. Lee, C. J. Creighton, A. R. Brannon, A. Luna, B. A. Aksoy, E. M. Liu, R. Shen, W. Lee, Y. Chen, S. M. Stirdivant, P. Russo, Y. B. Chen, S. K. Tickoo, V. E. Reuter, E. H. Cheng, C. Sander, and J. J. Hsieh. 2016. An Integrated Metabolic Atlas of Clear Cell Renal Cell Carcinoma. *Cancer Cell* **29**: 104-116.

9. Wiesener, M. S., P. M. Munchenhagen, I. Berger, N. V. Morgan, J. Roigas, A. Schwiertz, J. S. Jurgensen, G. Gruber, P. H. Maxwell, S. A. Loning, U. Frei, E. R. Maher, H. J. Grone, and K. U. Eckardt. 2001. Constitutive activation of hypoxia-inducible genes related to overexpression of hypoxia-inducible factor-1alpha in clear cell renal carcinomas. *Cancer Res* **61**: 5215-5222.

10. Haase, V. H. 2013. Regulation of erythropoiesis by hypoxia-inducible factors. *Blood Rev* **27**: 41-53.

11. Chan, D. A., P. D. Sutphin, P. Nguyen, S. Turcotte, E. W. Lai, A. Banh, G. E. Reynolds, J. T. Chi, J. Wu, D. E. Solow-Cordero, M. Bonnet, J. U. Flanagan, D. M. Bouley, E. E. Graves, W. A. Denny, M. P. Hay, and A. J. Giaccia. 2011. Targeting GLUT1 and the Warburg effect in renal cell carcinoma by chemical synthetic lethality. *Sci Transl Med* **3**: 94ra70.

12. Greijer, A. E., and E. van der Wall. 2004. The role of hypoxia inducible factor 1 (HIF-1) in hypoxia induced apoptosis. *J Clin Pathol* **57**: 1009-1014.

13. Velagapudi, S., M. Yalcinkaya, A. Piemontese, R. Meier, S. F. Norrelykke, D. Perisa, A. Rzepiela, M. Stebler, S. Stoma, P. Zanoni, L. Rohrer, and A. von Eckardstein. 2017. VEGF-A Regulates Cellular Localization of SR-BI as Well as Transendothelial Transport of HDL but Not LDL. *Arterioscler Thromb Vasc Biol*.

14. Kononen, J., L. Bubendorf, A. Kallioniemi, M. Barlund, P. Schraml, S. Leighton, J. Torhorst, M. J. Mihatsch, G. Sauter, and O. P. Kallioniemi. 1998. Tissue microarrays for high-throughput molecular profiling of tumor specimens. *Nat Med* **4**: 844-847.

15. Beleut, M., P. Zimmermann, M. Baudis, N. Bruni, P. Buhlmann, O. Laule, V. D. Luu, W. Gruissem, P. Schraml, and H. Moch. 2012. Integrative genome-wide expression profiling identifies three distinct molecular subgroups of renal cell carcinoma with different patient outcome. *BMC Cancer* **12**: 310.

16. Humphrey, P. A., H. Moch, A. L. Cubilla, T. M. Ulbright, and V. E. Reuter. 2016. The 2016 WHO Classification of Tumours of the Urinary System and Male Genital Organs-Part B: Prostate and Bladder Tumours. *Eur Urol* **70**: 106-119.

17. Rechsteiner, M. P., A. von Teichman, A. Nowicka, T. Sulser, P. Schraml, and H. Moch. 2011. VHL gene mutations and their effects on hypoxia inducible factor HIFalpha: identification of potential driver and passenger mutations. *Cancer Res* **71**: 5500-5511.

18. Struckmann, K., K. D. Mertz, S. Steu, M. Storz, P. Staller, W. Krek, P. Schraml, and H. Moch. 2008. pVHL co-ordinately regulates CXCR4/CXCL12 and MMP2/MMP9 expression in human clear-cell renal cell carcinoma. *The Journal of Pathology* **214**: 464-471.

19. Zhao, Y., H. Zhao, Y. Zhang, T. Tsatralis, Q. Cao, Y. Wang, Y. Wang, Y. M. Wang, S. I. Alexander, D. C. Harris, and G. Zheng. 2014. Isolation and epithelial co-culture of mouse renal peritubular endothelial cells. *BMC Cell Biology* **15**: 40.

20. Taub, M., B. U, L. Chuman, M. J. Rindler, M. H. Saier, Jr., and G. Sato. 1981. Alterations in growth requirements of kidney epithelial cells in defined medium associated with malignant transformation. *J Supramol Struct Cell Biochem* **15**: 63-72.

21. Hergovich, A., J. Lisztwan, R. Barry, P. Ballschmieter, and W. Krek. 2003. Regulation of microtubule stability by the von Hippel-Lindau tumour suppressor protein pVHL. *Nat Cell Biol* **5**: 64-70.

22. Ruf, M., C. Mittmann, A. M. Nowicka, A. Hartmann, T. Hermanns, C. Poyet, M. van den Broek, T. Sulser, H. Moch, and P. Schraml. 2015. pVHL/HIF-regulated CD70 expression is associated with infiltration of CD27+ lymphocytes and increased serum levels of soluble CD27 in clear cell renal cell carcinoma. *Clin Cancer Res* **21**: 889-898.

23. Casagrande, S., M. Ruf, M. Rechsteiner, L. Morra, S. Brun-Schmid, A. von Teichman, W. Krek, P. Schraml, and H. Moch. 2013. The protein tyrosine phosphatase receptor type J is regulated by the pVHL-HIF axis in clear cell renal cell carcinoma. *J Pathol* **229**: 525-534.

24. Havel, R. J., H. A. Eder, and J. H. Bragdon. 1955. The distribution and chemical composition of ultracentrifugally separated lipoproteins in human serum. *The Journal of clinical investigation* **34**: 1345-1353.

25. Rohrer, L., C. Cavelier, S. Fuchs, M. A. Schluter, W. Volker, and A. von Eckardstein. 2006. Binding, internalization and transport of apolipoprotein A-I by vascular endothelial cells. *Biochim Biophys Acta* **1761**: 186-194.

26. Freeman, M., Y. Ekkel, L. Rohrer, M. Penman, N. J. Freedman, G. M. Chisolm, and M. Krieger. 1991. Expression of type I and type II bovine scavenger receptors in Chinese hamster ovary cells: lipid droplet accumulation and nonreciprocal cross competition by acetylated and oxidized low density lipoprotein. *Proc Natl Acad Sci U S A* **88**: 4931-4935.

27. Goldstein, J. L., G. Y. Brunschede, and M. S. Brown. 1975. Inhibition of proteolytic degradation of low density lipoprotein in human fibroblasts by chloroquine, concanavalin A, and Triton WR 1339. *J Biol Chem* **250**: 7854-7862.

28. Keidar, S., G. J. Brook, M. Rosenblat, B. Fuhrman, G. Dankner, and M. Aviram. 1992. Involvement of the macrophage low density lipoprotein receptor-binding domains in the uptake of oxidized low density lipoprotein. *Arterioscler Thromb* **12**: 484-493.

29. Ong, A. C., and J. F. Moorhead. 1994. Tubular lipidosis: epiphenomenon or pathogenetic lesion in human renal disease? *Kidney Int* **45**: 753-762.

30. Goldstein, J. L., and M. S. Brown. 2009. The LDL receptor. *Arterioscler Thromb Vasc Biol* **29**: 431-438.

31. Chen, W. J., J. L. Goldstein, and M. S. Brown. 1990. NPXY, a sequence often found in cytoplasmic tails, is required for coated pit-mediated internalization of the low density lipoprotein receptor. *J Biol Chem* **265**: 3116-3123.

32. Davis, C. G., J. L. Goldstein, T. C. Sudhof, R. G. Anderson, D. W. Russell, and M. S. Brown. 1987. Acid-dependent ligand dissociation and recycling of LDL receptor mediated by growth factor homology region. *Nature* **326**: 760-765.

33. Lambert, G., B. Sjouke, B. Choque, J. J. Kastelein, and G. K. Hovingh. 2012. The PCSK9 decade. *J Lipid Res* **53**: 2515-2524.

34. Skrzydlewski, Z., and K. Worowski. 1978. Degradation of low-density lipoproteins (LDL) and LDL - protamine complexes by lysosomal protease. *Acta Biol Acad Sci Hung* **29**: 19-22.

35. Linke, M., R. E. Gordon, M. Brillard, F. Lecaille, G. Lalmanach, and D. Bromme. 2006. Degradation of apolipoprotein B-100 by lysosomal cysteine cathepsins. *Biol Chem* **387**: 1295-1303.

36. Goldstein, J. L., S. E. Dana, J. R. Faust, A. L. Beaudet, and M. S. Brown. 1975. Role of lysosomal acid lipase in the metabolism of plasma low density lipoprotein. Observations in cultured fibroblasts from a patient with cholesteryl ester storage disease. *J Biol Chem* **250**: 8487-8495.

37. Soccio, R. E., and J. L. Breslow. 2004. Intracellular cholesterol transport. *Arterioscler Thromb Vasc Biol* **24**: 1150-1160.

38. Go, G. W., and A. Mani. 2012. Low-density lipoprotein receptor (LDLR) family orchestrates cholesterol homeostasis. *Yale J Biol Med* **85**: 19-28.

39. Boysen, G., D. Bausch-Fluck, C. R. Thoma, A. M. Nowicka, D. P. Stiehl, I. Cima, V. D. Luu, A. von Teichman, T. Hermanns, T. Sulser, B. Ingold-Heppner, N. Fankhauser, R. H. Wenger, W. Krek, P. Schraml, B. Wollscheid, and H. Moch. 2012. Identification and functional characterization of pVHL-dependent cell surface proteins in renal cell carcinoma. *Neoplasia* **14**: 535-546.

40. Acton, S. L., P. E. Scherer, H. F. Lodish, and M. Krieger. 1994. Expression cloning of SR-BI, a CD36-related class B scavenger receptor. *J Biol Chem* **269**: 21003-21009.

41. Pagler, T. A., S. Rhode, A. Neuhofer, H. Laggner, W. Strobl, C. Hinterndorfer, I. Volf, M. Pavelka, E. R. Eckhardt, D. R. van der Westhuyzen, G. J. Schutz, and H. Stangl. 2006. SR-BI-mediated high density lipoprotein (HDL) endocytosis leads to HDL resecretion facilitating cholesterol efflux. *J Biol Chem* **281**: 11193-11204.

42. Rohrer, L., P. M. Ohnsorg, M. Lehner, F. Landolt, F. Rinninger, and A. von Eckardstein. 2009. High-density lipoprotein transport through aortic endothelial cells involves scavenger receptor BI and ATP-binding cassette transporter G1. *Circ Res* **104**: 1142-1150.

43. Armstrong, S. M., M. G. Sugiyama, K. Y. Fung, Y. Gao, C. Wang, A. S. Levy, P. Azizi, M. Roufaiel, S. N. Zhu, D. Neculai, C. Yin, S. S. Bolz, N. G. Seidah, M. I. Cybulsky, B. Heit, and W. L. Lee. 2015. A novel assay uncovers an unexpected role for SR-BI in LDL transcytosis. *Cardiovasc Res* **108**: 268-277.

44. Eckhardt, E. R., L. Cai, B. Sun, N. R. Webb, and D. R. van der Westhuyzen. 2004. High density lipoprotein uptake by scavenger receptor SR-BII. *J Biol Chem* **279**: 14372-14381.

45. Eckhardt, E. R., L. Cai, S. Shetty, Z. Zhao, A. Szanto, N. R. Webb, and D. R. Van der Westhuyzen. 2006. High density lipoprotein endocytosis by scavenger receptor SR-BII is clathrin-dependent and requires a carboxyl-terminal dileucine motif. *J Biol Chem* **281**: 4348-4353.

46. Saddar, S., C. Mineo, and P. W. Shaul. 2010. Signaling by the high-affinity HDL receptor scavenger receptor B type I. *Arterioscler Thromb Vasc Biol* **30**: 144-150.

47. Lim, H. Y., C. H. Thiam, K. P. Yeo, R. Bisoendial, C. S. Hii, K. C. McGrath, K. W. Tan, A. Heather, J. S. Alexander, and V. Angeli. 2013. Lymphatic vessels are essential for the removal of cholesterol from peripheral tissues by SR-BI-mediated transport of HDL. *Cell Metab* **17**: 671-684.

48. Fung, K. Y., C. Wang, S. Nyegaard, B. Heit, G. D. Fairn, and W. L. Lee. 2017. SR-BI Mediated Transcytosis of HDL in Brain Microvascular Endothelial Cells Is Independent of Caveolin, Clathrin, and PDZK1. *Front Physiol* **8**: 841.

49. Zachary, I., and G. Gliki. 2001. Signaling transduction mechanisms mediating biological actions of the vascular endothelial growth factor family. *Cardiovasc Res* **49**: 568-581.

50. Cao, Y., L. Wang, D. Nandy, Y. Zhang, A. Basu, D. Radisky, and D. Mukhopadhyay. 2008. Neuropilin-1 upholds dedifferentiation and propagation phenotypes of renal cell carcinoma cells by activating Akt and sonic hedgehog axes. *Cancer Res* **68**: 8667-8672.

51. Beloribi-Djefaflia, S., S. Vasseur, and F. Guillaumond. 2016. Lipid metabolic reprogramming in cancer cells. *Oncogenesis* **5**: e189.

52. Xu, G., N. Lou, Y. Xu, H. Shi, H. Ruan, W. Xiao, L. Liu, H. Xiao, B. Qiu, L. Bao, C. Yuan, K. Chen, H. Yang, and X. Zhang. 2017. Diagnostic and prognostic value of scavenger receptor class B type 1 in clear cell renal cell carcinoma. *Tumour Biol* **39**: 1010428317699110.

53. Pospiech, E., J. Ligeza, W. Wilk, A. Golas, J. Jaszczynski, A. Stelmach, J. Rys, A. Blecharczyk, A. Wojas-Pelc, J. Jura, and W. Branicki. 2015. Variants of SCARB1 and VDR Involved in Complex Genetic Interactions May Be Implicated in the Genetic Susceptibility to Clear Cell Renal Cell Carcinoma. *Biomed Res Int* **2015**: 860405.

54. Kinslechner, K., D. Schorghofer, B. Schutz, M. Vallianou, B. Wingelhofer, W. Mikulits, C. Rohrl, M. Hengstschlager, R. Moriggl, H. Stangl, and M. Mikula. 2018. Malignant Phenotypes in Metastatic Melanoma are Governed by SR-BI and its Association with Glycosylation and STAT5 Activation. *Mol Cancer Res* **16**: 135-146.

55. Hoekstra, M., and M. Sorci-Thomas. 2017. Rediscovering scavenger receptor type BI: surprising new roles for the HDL receptor. *Curr Opin Lipidol* **28**: 255-260.

Table 1

Protein of interest	Staining intensity	Subtype		
		Clear-cell RCC	Chromophobe	Papillary
apoA-I	**0 (n)**	5.1% (9)	0	12% (3)
	1 (n)	18.9% (33)	50% (3)	44% (11)
	2 (n)	24.6% (43)	16.7% (1)	32% (8)
	3 (n)	51.4% (90)	33.3% (2)	12% (3)
apoB	**0 (n)**	21.7% (38)	16.7% (1)	24% (6)
	1 (n)	62.3% (109)	50% (3)	68% (17)
	2 (n)	16% (28)	33.3% (2)	8% (2)
SR-BI	**0 (n)**	18.7% (31)	80% (4)	78.9% (15)
	1 (n)	25.3% (42)	20% (1)	10.5 (2)
	2 (n)	27.7% (46)	0	5.3 (1)
	3 (n)	28.3% (47)	0	5.3 (1)

Table 1: Quantification of apolipoproteins and SR-BI expression in renal cell carcinoma TMA Percent and absolute (n = number) frequencies of anti-apoA-I, anti-apoB and anti-SR-BI staining intensities among renal cell carcinoma subtypes.

Figure 1

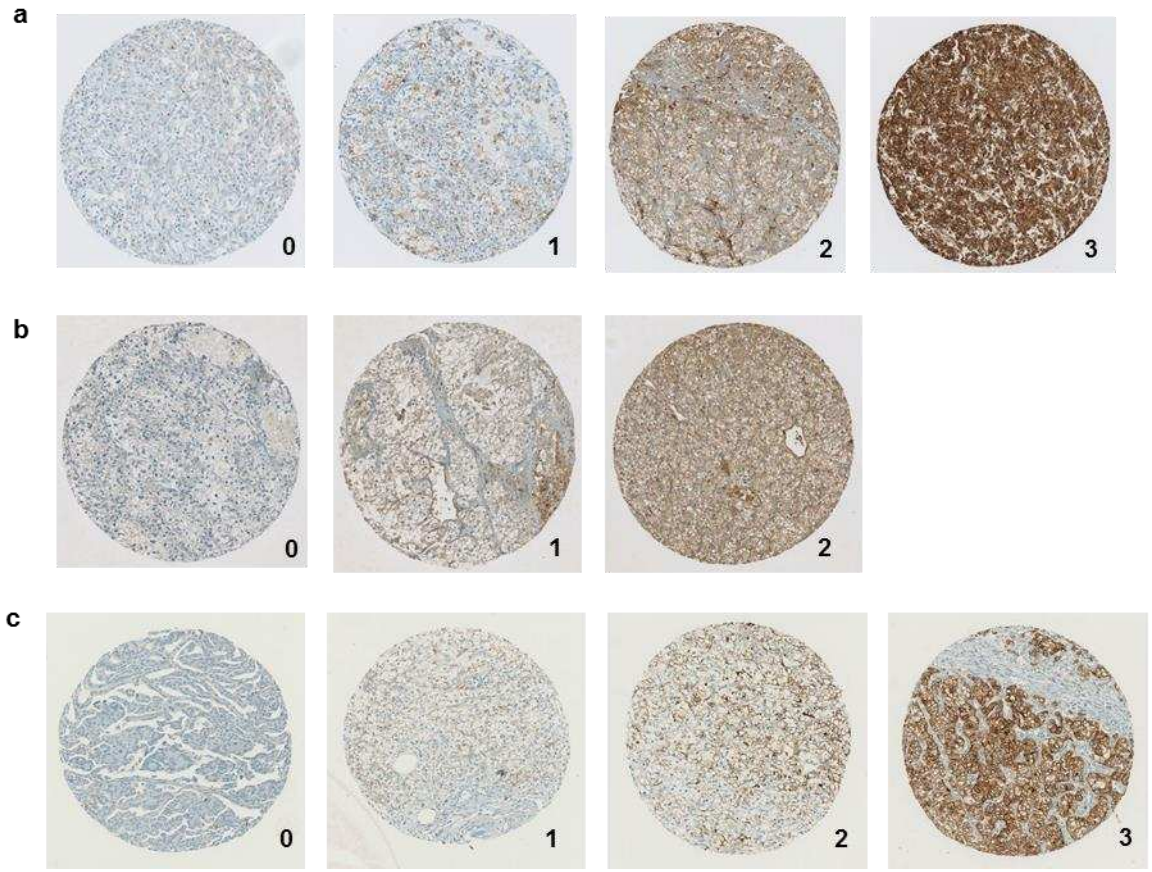

Figure 1: Apolipoprotein and SR-BI expression in renal cell carcinoma TMA Immunostaining of **a**, apoA-I **b**, apoB and **c**, SR-BI of human tissue microarrays. The grading from 0-3 represents the staining intensity from negative to the strongest.

Figure 2

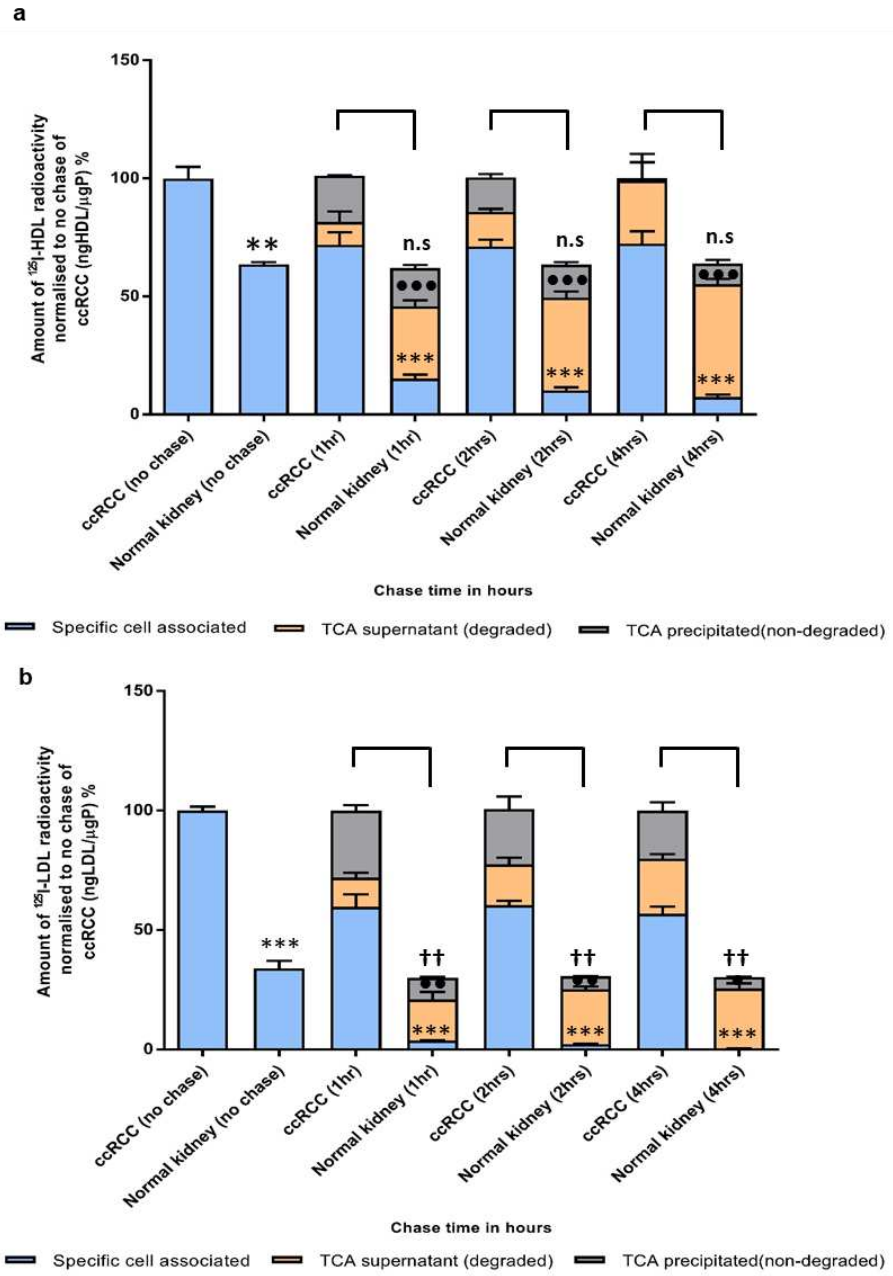

Figure 2 Cellular association, resecretion and degradation of ^{125}I-HDL and ^{125}I-LDL in patient-derived ccRCC and normal kidney epithelial cell cultures. Both ccRCC- and normal kidney derived cells were pulsed for 1 hour with 10µg/mL of either **a,** ^{125}I-HDL or **b,** ^{125}I-LDL at 37ºC in the absence (total) or in the presence of 40-fold excess of unlabeled HDL or LDL (unspecific). Subsequently, the cells were either lysed and analyzed for their content of radiolabel or chased for 1,2 and 4 hours with unlabeled HDL or LDL at 37ºC. The media were collected and subjected to precipitation with TCA to count radioactivity of non-degraded /resecreted lipoproteins in the precipitate and degraded lipoproteins in the supernatant separately. Specific association was calculated by subtracting unspecific values from total values. The amount of radioactivity in each fraction of the well (cell associated, TCA supernatant and TCA precipitated) was calculated by normalizing to the specific cellular association of the no chase of ccRCC cells (represents initial radioactivity for the chase points). The results are represented as mean±s.e.m of two independent experiments, with two batches of ^{125}I-HDL and ^{125}I-LDL. Significance is determined for each fraction at each time point using by Mann-Whitney test. For specific cell associated: *** $P \leq 0.001$. For TCA supernatant: •••$P \leq 0.001$, ••$P \leq 0.01$, •$P \leq 0.05$. For TCA precipitated: †† $P \leq 0.01$, †$P \leq 0.05$. n.s represents "not significant".

Figure 3

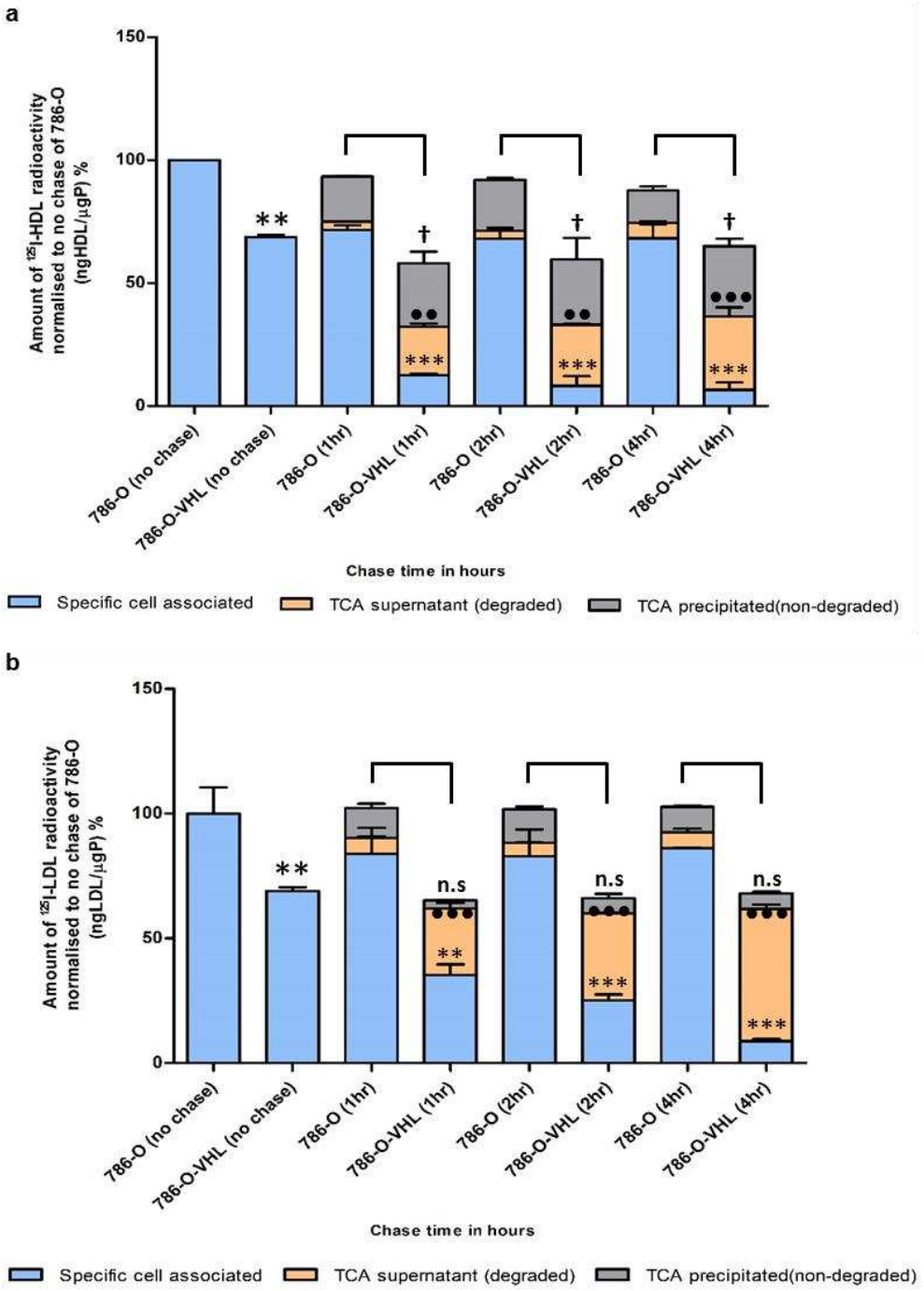

Figure 3: Cellular association, re-secretion and degradation of ^{125}I-HDL and ^{125}I-LDL in 786-O and 786-O-VHL cells. The results are represented as mean±s.e.m of two independent experiments, with two batches of ^{125}I-HDL and ^{125}I-LDL which were performed as described in the legend of Figure 2. Significance is determined for each fraction at each time point using by Mann-Whitney test. For specific cell associated: *** $P \leq 0.001$, ** $P \leq 0.01$. For TCA supernatant: ●●●$P \leq 0.001$, ●●$P \leq 0.01$. For TCA precipitated: †$P \leq 0.05$. n.s represents "not significant".

Figure 4

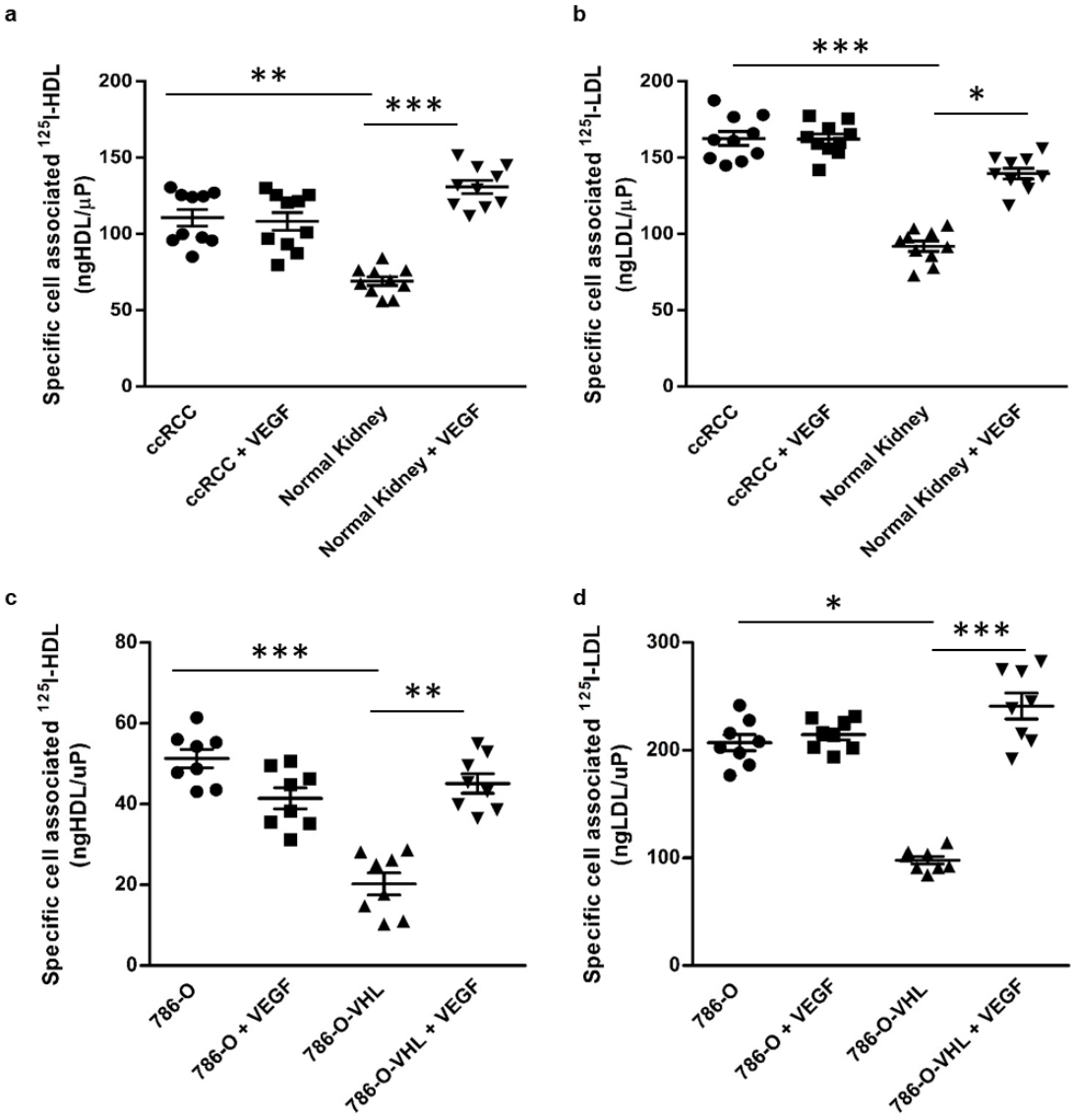

Figure 4: Loss of VHL promotes cellular association of ^{125}I-HDL and ^{125}I-LDL in ccRCC cells Patient-derived ccRCC and normal epithelial kidney cell cultures, 786-O and 786-O-VHL cells were pre-treated with 25ng/mL of VEGF for 1 hour prior to assays, followed by incubation with 10µg/mL of **a, c** ^{125}I-HDL or **b, d** ^{125}I-LDL at 37 ºC for 1 hour in the absence (total) or in the presence of 40-fold excess of unlabeled HDL or LDL (unspecific). Specific cellular association was calculated by subtracting unspecific values from total values. The results are represented as mean±s.e.m of three independent experiments (in triplicates, triplicates and duplicates respectively) for cell lines and two independent experiments with patient-derived cells, with two batches of ^{125}I-HDL and ^{125}I-LDL. Significance is determined by Kruskal-Wallis test followed by Dunn's post-test. ***$P \leq 0.001$, **$P \leq 0.01$, *$P \leq 0.05$.

Figure 5

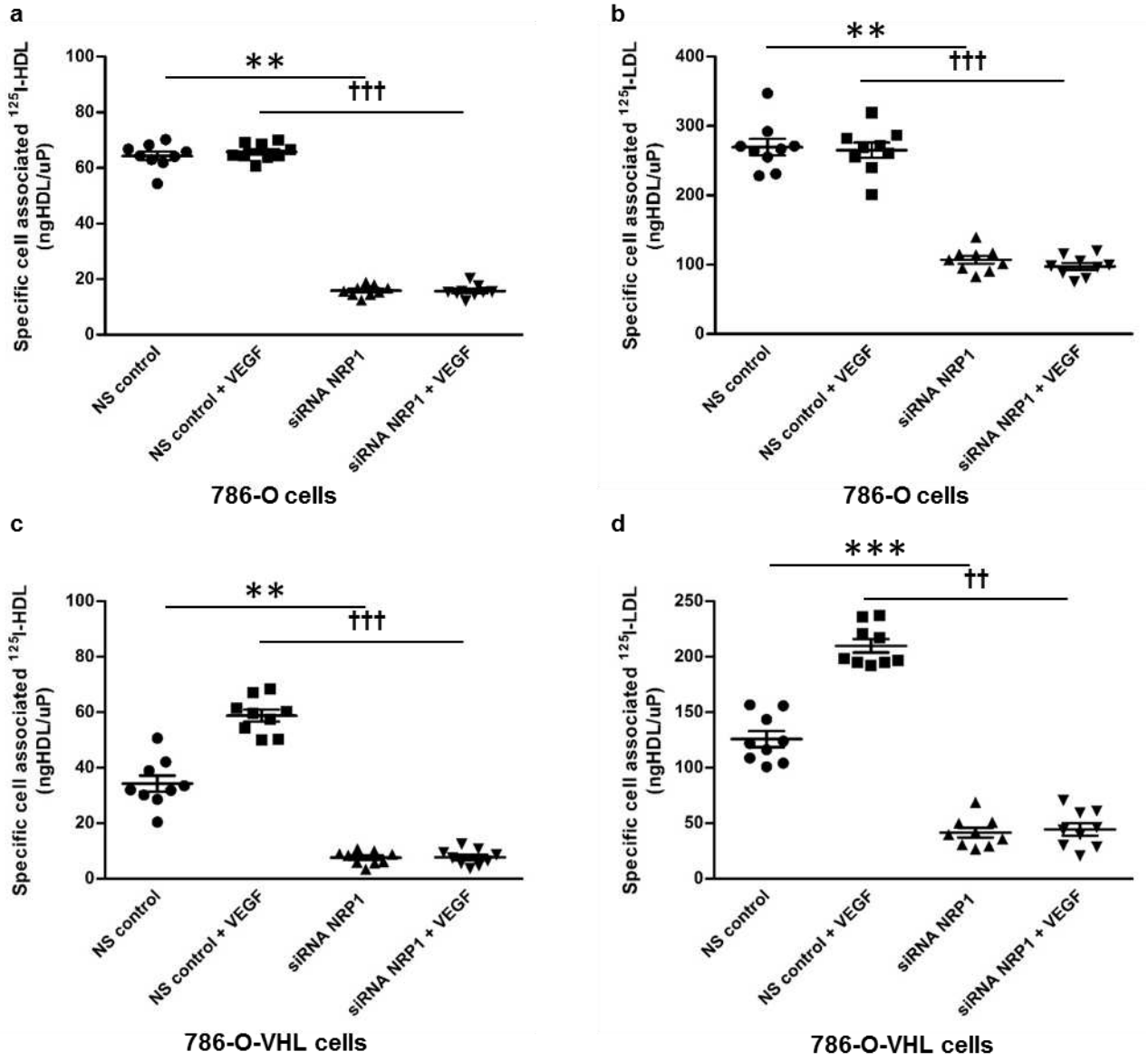

Figure 5: NRP1 promotes cellular association of ^{125}I-HDL and ^{125}I-LDL in renal carcinoma 786-O cells 786-O and 786-O-VHL cells were transfected with specific siRNA against NRP1 or with non-silencing control siRNA (NS control). After 72 hours of transfection, the cells were pre-treated with 25ng/ml of VEGF for 1 hour prior to assays as indicated, followed by incubation with 10µg/mL of ^{125}I-HDL or ^{125}I-LDL. 786-O cells incubated with **a,** ^{125}I-HDL **b,** ^{125}I-LDL. 786-O-VHL cells incubated with **c,** ^{125}I-HDL **d,** ^{125}I-LDL at 37 ℃ for 1 hour in the absence (total) or in the presence of 40-fold excess of unlabeled HDL or LDL (unspecific). Specific cellular association was calculated by subtracting unspecific values from total values. The results are represented as mean±s.e.m of three independent experiments (each experiment in triplicates), with two batches of ^{125}I-HDL and ^{125}I-LDL. Significance is determined by Kruskal-Wallis test followed by Dunn's post-test. ***$P \leq 0.001$, **$P \leq 0.01$, †††$P \leq 0.001$, ††$P \leq 0.01$.

Figure 6

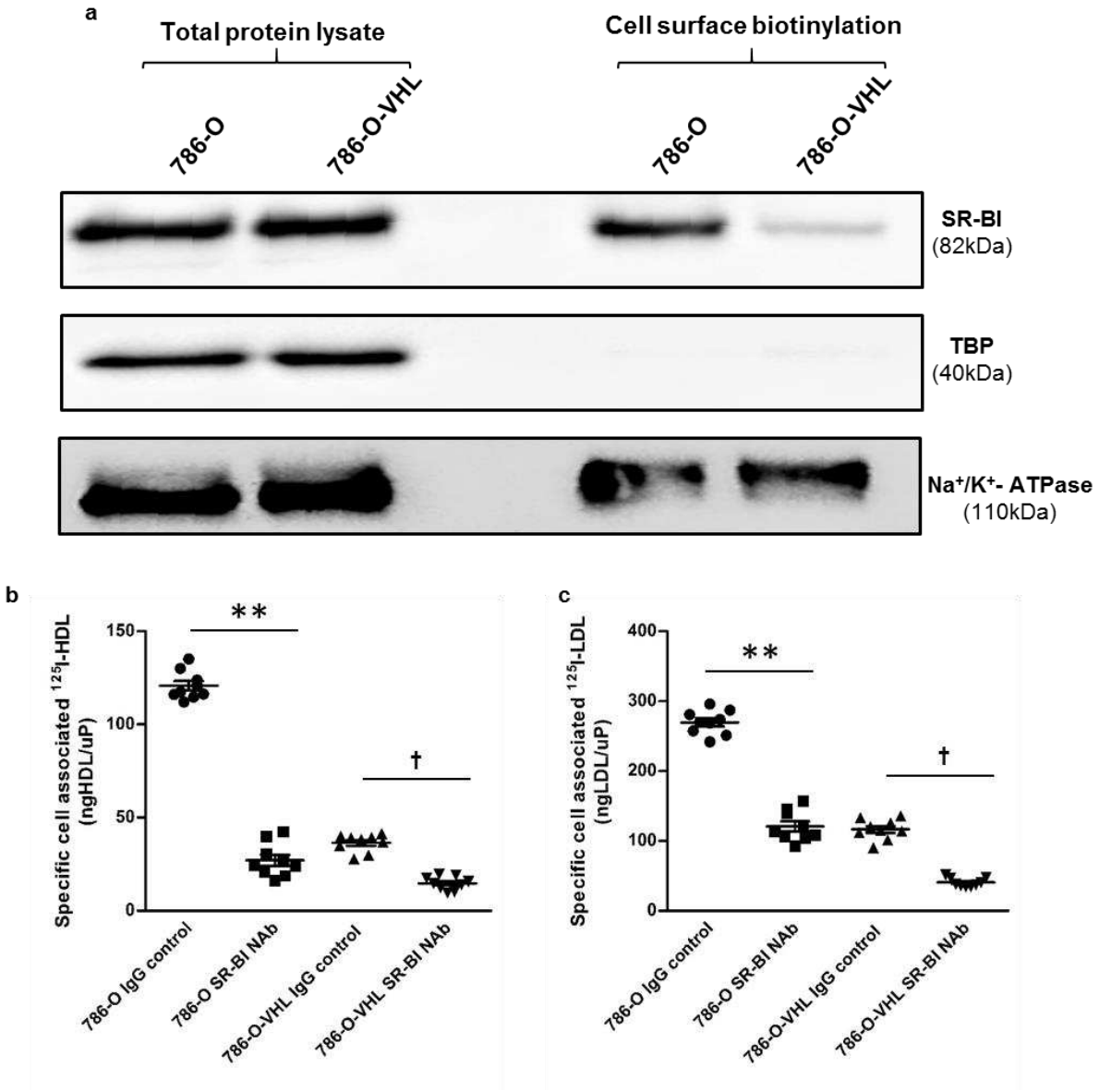

Figure 6: SR-BI mediates cellular association of ^{125}I-HDL and ^{125}I-LDL in 786-O cells a, Cell surface expression of SR-BI in renal carcinoma cells. Western blot analysis of SR-BI in total cell lysates (left) and on the cell surface (right) in 786-O and 786-O-VHL cells. The western blots were probed with anti-SR-BI (82kDa) and anti-TBP (40kDa, used as a control for intracellular protein expression), anti Na^+/K^+-ATPase (110kDa, used as a control for cell surface protein expression). 786-O and 786-O-VHL cells were pre-treated with either anti-SR-BI neutralizing antibody or isotype (IgG) control for 1 hour prior to assays, followed by incubation with 10µg/mL of **b,** ^{125}I-HDL or **c,** ^{125}I-LDL for 1 hour in the absence (total) or in the presence of 40-fold excess of unlabeled HDL or LDL (unspecific) at 37 ºC. Specific association was calculated by subtracting unspecific values from total values. The results are represented as mean±s.e.m of three independent experiments (each experiment in triplicates) with two batches of ^{125}I-HDL and ^{125}I-LDL. Significance is determined by Kruskal-Wallis test followed by Dunn's post-test. IgG control represents isotype control and anti-SR-BI Nab represents treatment with SR-BI neutralizing antibody. $^{**}P \leq 0.01$, $\dagger P \leq 0.05$. Complete blots in Supplementary Electrophoretic Blot A.

Figure 7

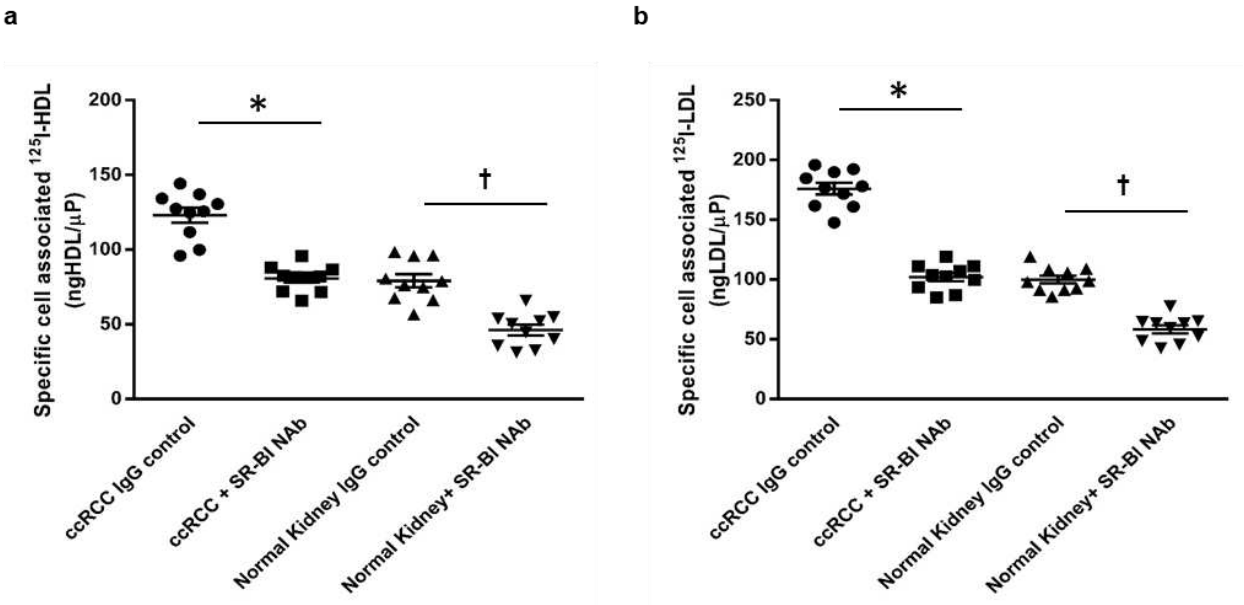

Figure 7: SR-BI mediates cellular association of ^{125}I-HDL and ^{125}I-LDL in ccRCC cells Both the patient-derived ccRCC and normal epithelial kidney cell cultures were pre-treated with either anti-SR-BI neutralizing antibody or isotype (IgG) control for 1 hour prior to assays, followed by incubation with 10μg/mL of **a,** ^{125}I-HDL or **b,** ^{125}I-LDL for 1 hour in the absence (total) or in the presence of 40-fold excess of unlabeled HDL or LDL (unspecific) at 37 ºC. Specific association was calculated by subtracting unspecific values from total values. The results are represented as mean±s.e.m of two independent experiments (each experiment in triplicates) with two batches of ^{125}I-HDL and ^{125}I-LDL. Significance is determined by Kruskal-Wallis test followed by Dunn's post-test. IgG control represents isotype control and anti-SR-BI Nab represents treatment with SR-BI neutralizing antibody. *$P \leq 0.05$, †$P \leq 0.05$.

JOURNAL OF LIPID RESEARCH ASBMB

Figure 8

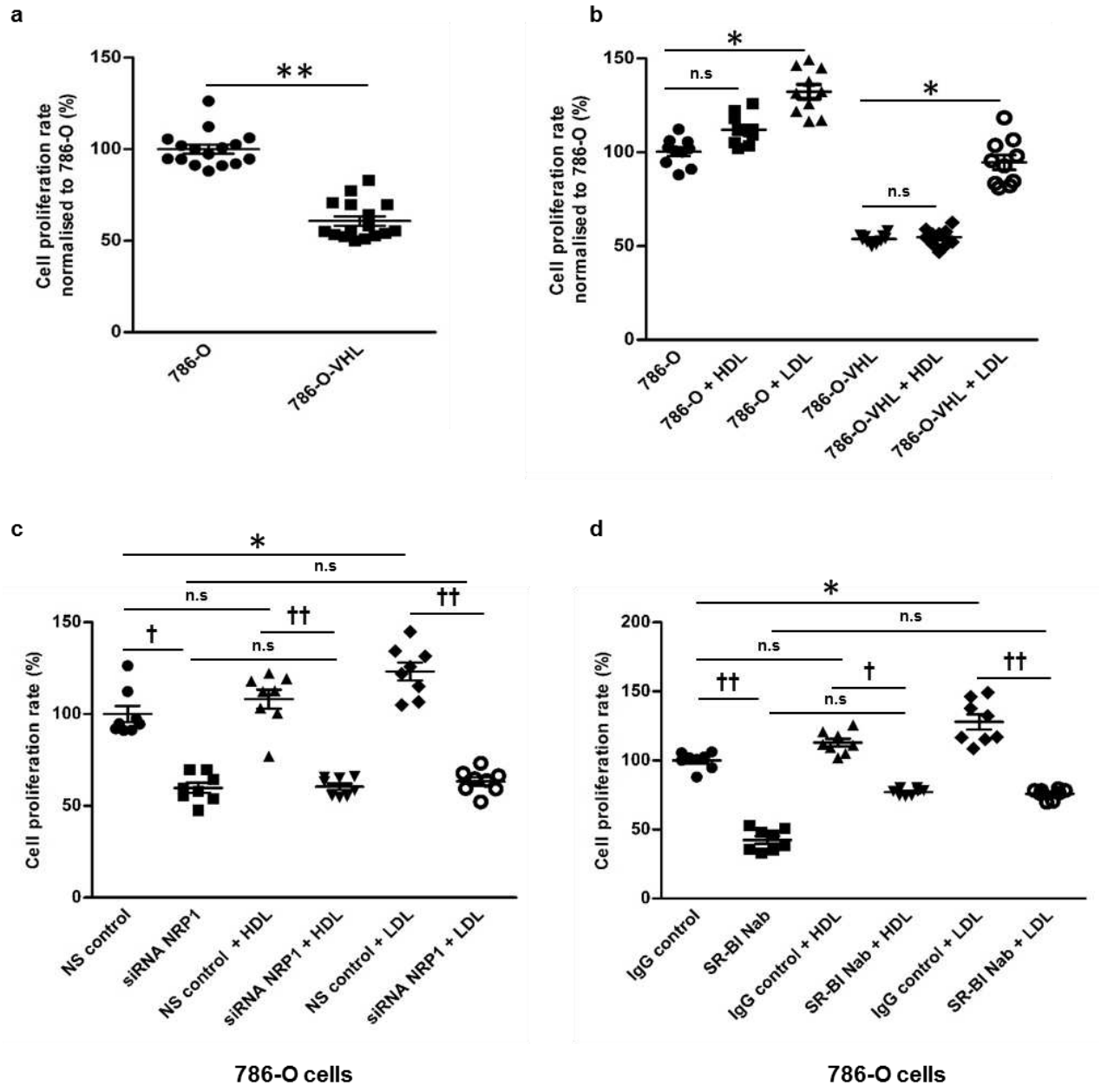

Figure 8: Effects of VHL, HDL, LDL, NRP1 and SR-BI on proliferation of ccRCC cells. VHL-defective 786-O and VHL-intact 786-O-VHL cells were cultured in a 96 well plate for 60 hours prior to the overnight treatment with 50µg/mL of HDL or LDL. The rate of proliferation was analyzed using the MTT assay. **a,** comparison of 786-O and 786-O-VHL cells per se **b**, in the presence or absence of 50µg/mL of either HDL or LDL. 786-O cells were transfected with **c,** specific siRNA against NRP1 or with non-silencing control siRNA (NS control) for 60 hours or **d**, pre-treated with a neutralizing antiSR-BI antibody for 1 hour prior to the overnight treatment with 50µg/mL of HDL or LDL. The results are represented as mean±s.e.m of three independent experiments with two batches of HDL and LDL. Significance is determined by Kruskal-Wallis test followed by Dunn's post-test. IgG control represents isotype control and anti-SR-BI Nab represents treatment with neutralizing anti-SR-BI antibody. ***$P \leq 0.001$, **$P \leq 0.01$, *$P \leq 0.05$. †††$P \leq 0.001$, ††$P \leq 0.01$, †$P \leq 0.05$ and ns represents "not significant".